ingegneria sismica
International Journal of Earthquake Engineering
Anno XLIII - Num. 2 - 2026

Hybrid Neural Networks for Real-Time Arrhythmia Detection and Blood Pressure Trend Prediction in Wearable Monitoring Systems

Wenshan Chen[1,*], *Peisong Ye*[2] *and Xiuling Jiang*[3]

[1] School of Medical Technology and Engineering, Fujian Health College, Fuzhou, Fujian, 350101, China
[2] Fujian Provincial Hospital, Fuzhou University, Fuzhou, Fujian, 350001, China
[3] Department of Social Sports, Fujian Sports Vocational Education and Technical College, Fuzhou, Fujian, 350003, China

SUMMARY: *In light of the escalating global mortality rate attributed to cardiovascular diseases, wearable devices designed for real - time tracking of human physiological data are making rapid inroads. Acoustic sensors, thanks to their low energy consumption, compact dimensions, and cost - effectiveness, are extensively employed in the detection of human physiological states.To begin with, we leverage a convolutional neural network to analyze the morphological characteristics of electrocardiogram (ECG) signals. By using a bidirectional long - short - term memory network, we capture the contextual relationships within these features and develop a CNN - BLSTM network model. Next, we carry out label marking, derived signal extraction, and noise elimination on photoplethysmogram (PPG) signals. We further refine the CNN - BiLSTM model by incorporating an attention mechanism module to achieve blood pressure detection.The experimental findings indicate that the CNN - BiLSTM network model boosts the classification accuracy in class S and class F by 2.02% and 12.94% respectively. Additionally, the recall rate improves by 12.94% and 4.11% respectively, fulfilling the criteria for arrhythmia detection. On the dataset, the optimized CNN - BiLSTM blood pressure prediction model attains a systolic mean error (ME) of 0.8429 mmHg, a mean absolute error (MAE) of 4.5916 mmHg, and a root - mean - square error (RMSE) of 7.1219 mmHg. For diastolic blood pressure, the predicted ME is 2.2577 mmHg and the MAE is 3.0081 mmHg.Lastly, a wearable system capable of simultaneously monitoring blood pressure and atrial fibrillation is developed. This system offers technical backing and practical strategies for the application of wearable medical devices in real - time cardiovascular health monitoring situations.*

KEYWORDS: *Convolutional neural net; Bidirectional long - and short - term memory net; ECG signal; monitoring system; blood pressure prediction*

1 Introduction

As the social economy progresses and the national way of life undergoes constant alterations, particularly with the aging of the population and the rapid pace of urbanization, the unhealthy living habits of residents are becoming increasingly evident. This has led to a continuous rise in the incidence of cardiovascular diseases[1, 2]. Arrhythmias and blood pressure changes often precede or accompany cardiovascular disease, so early detection of cardiovascular disease has

*wschen2026@126.com
https://doi.org/10.65102/is2026601
Published: 30 April, 2026

a certain amount of preventive effect, for the later treatment can also provide an effective basis [3, 4]. Although traditional electrocardiographs can measure 12-lead electrocardiograms, they are bulky and require the use of medical electrode patches, which are not suitable for long-term wear [5, 6]. With the rapid progress of information technology, wearable monitoring systems have been developed more rapidly and continue to meet the needs of the public for a healthy life [7].

A wearable monitoring system utilizes multimedia, wireless communication, and sensor technologies to gather a wide range of physiological metrics of the human body. The purpose of this system is to achieve the monitoring of diverse human vital signs, which encompasses the detection of arrhythmia and the prediction of blood pressure trends [8-10]. Its wearability allows users to use it at any time in any exercise state without going to the hospital. As artificial intelligence advances, to enhance the precision and sophistication of wearable monitoring systems, the incorporation of hybrid neural networks has emerged as a crucial avenue for their development [11, 12].

A neural network is a computational construct designed to replicate the human brain's neural system. It is composed of a collection of interconnected neuron - like units. These units are capable of transmitting and processing data. Through study and training, neural networks can gain the ability to comprehend and address various problems [13-15]. Hybrid neural networks, on the other hand, are composite models that combine multiple neural network architectures, which are capable of solving more complex tasks [16]. Within wearable monitoring systems, integrated neural networks offer resolutions for the intelligence of these systems. They enhance cardiovascular health management by leveraging neural networks and long - short - term memory networks. These networks are used to extract spatial characteristics and detect temporal correlations. As a result, they can efficiently and precisely classify arrhythmias and forecast continuous trends in blood pressure [17-20].

This paper presents an arrhythmia detection model that combines a one - dimensional convolutional neural network and a bidirectional long - and short - term memory network. The model capitalizes on the strengths of the convolutional neural network, which is robust against noise, and the long - and short - term memory network's proficiency in handling time - series data. To begin with, the wavelet approach is employed to reduce noise in electrocardiogram (ECG) signals. Subsequently, detection experiments are conducted on the MIT - BIH arrhythmia dataset.For photoplethysmogram (PPG) signals, label assignment, derived signal extraction, and noise management are carried out. The Tsfresh technique is then used to extract signal features. To predict blood pressure trends, an attention mechanism is incorporated to fine - tune the CNN - BiLSTM model.

2 Basics of hybrid neural networks

2.1 Convolutional Neural NetworksCrucial

Convolutional Neural Networks (CNNs) are applicable for feature learning on extensive - scale datasets to distill features. They process data by successively applying convolution and pooling operations across different layers. A simple CNN is composed of convolutional, pooling, and fully - connected layers. In contrast, a sophisticated CNN is formed by various network structures interlocked with one another.

The convolutional layer makes use of weight sharing and local connectivity to carry out convolution on the input data, aiming to extract profound features. Typically, it comprises numerous learnable convolution filters. When data features undergo convolution with the convolution filters, it indicates that a dot product operation is executed between the input data

and the filters. Subsequently, the outcome is input into the activation function to generate the output features. The output value a_j^l of the j th cell of the convolutional layer l is calculated as follows:

$$a_j^l = f\left(b_j^l + \sum_{i \in M_j^l} a_i^{l-1} * k_{ij}^l\right) \tag{1}$$

where: M_j^l - the set of features for selecting inputs; k - learnable convolution kernel; * - dot product operation.

The pooling layer conducts pooling operations on the data that has been processed by the convolutional layer according to specific rules. This is done to decrease the quantity of parameters, preserve the primary features, and avoid overfitting. Typically, it comes after the convolutional layer, and there is a one - to - one correspondence between each convolutional layer and pooling layer. The calculation of the activation value a_j^l within pooling layer l is as follows:

$$a_j^l = f\left(b_j^l + \beta_j^l down\left(a_j^{l-1}, M^l\right)\right) \tag{2}$$

where $down(\cdot)$ denotes the pooling function, commonly used pooling functions are mean pooling, maximum pooling, minimum pooling, random pooling, etc., b_j^l is the bias, β_j^l is the multiplicative residual, and M^l denotes that the size of the pooling frame used in the l th layer is $M^l \times M^l$.

The fully connected layer is mainly for the convenience of the model output, which is followed by a connected output layer or a multi-layer fully connected structure. The feature mappings from the previous layer are combined into a higher level representation and eventually used to perform classification, regression or other tasks. This has enabled CNNs to excel in image processing, natural language processing and other fields.

CNNs are powerful tools for dealing with time series anomaly detection problems, effectively extracting key features from time series data, with convolutional operations able to capture local dependencies in time series data, and parameter sharing mechanisms allowing the model to efficiently process long time series data. The convolutional layer captures local patterns in the data, while the pooling layer reduces the dimensionality of the data.

2.2 Long and short-term memory networks

Recurrent neural network (RNN) is one of the earliest machine learning models used for time series prediction, while long short-term memory network (LSTM) is an improved version of RNN, which is able to solve the gradient vanishing problem that exists in RNN well.LSTM can effectively preserve the features of time-series data by introducing a gate structure to control the information transfer.The recurrent unit structure of LSTM includes the forgetting gate f_t, input gate i_t, and output gate o_t, which are the three key gate control structures. Through these gates, LSTM can selectively forget or preserve the past information and add new information to achieve effective feature extraction and modeling of timing data.

The computational process of LSTM is as follows:

(1) Forgetting gate:

$$f_t = \sigma\left(\omega_f \cdot [h_{t-1}, x_t] + b_f\right) \tag{3}$$

where: f_t - output of the forgetting gate; ω_f - coefficient matrix; b_f - bias vector.

(2) Input gate:

$$i_t = \sigma\left(\omega_i \cdot [h_{t-1}, x_t] + b_i\right) \tag{4}$$

$$\tilde{C}_t = \tanh\left(\omega_C \cdot [h_{t-1}, x_t] + b_C\right) \tag{5}$$

where: i_t - sigma activation function output; $\tilde{C}_t$ - tanh activation function output; ω_i, ω_C - the - coefficient matrix; b_i, b_C - bias vector.

Cell state:

$$C_t = f_t \odot C_{t-1} + i_t \odot \tilde{C}_t \tag{6}$$

where: C_t - the state of the cell; $\odot$ represents the Hadamard product.

(3) Output gate:

$$o_t = \sigma\left(\omega_o \cdot [h_{t-1}, x_t] + b_o\right) \tag{7}$$

$$h_t = o_t \odot \tanh\left(C_t\right) \tag{8}$$

where: o_t - output of the output gate; ω_o - coefficient matrix; b_o - bias vector; h_t -- the outcome generated by the concealed layer.

LSTM can effectively capture temporal correlations in data, including trend, seasonality and periodicity, etc. It can effectively integrate time-series information and simultaneously process inputs from different time steps to better capture anomalies in time series.

3 Real-time arrhythmia detection based on CNN-BiLSTM

3.1 Data preprocessing and representation

In existing arrhythmia classification studies, the preprocessing process usually includes filtering operations such as wavelet transform or filter bank to obtain clean ECG data. In order to preserve the original features of the ECG signal as much as possible to increase the Existing arrhythmia classification studies, the preprocessing process usually includes filtering operations such as wavelet transform or filter bank to obtain clean ECG data. To ensure consistent input shape, each beat obtained from the processing is unified into a data segment with a length of 261 sample points.

The preprocessed beats $X = [x_1, x_2, \cdots, x_n]$ are used as inputs to the network, where n is 261. The input X corresponds to the label $y \in \{N, S, V, F, Q\}$.

3.2 CNN-BLSTM network models

3.2.1 Convolutional Neural Network Module

As depicted in Figure 1, the convolutional neural network component is composed of multiple convolutional layers, pooling layers, and other operations. The convolutional layers possess characteristics like local connectivity and weight sharing, which are utilized to extract local features of one - dimensional electrocardiogram (ECG) signals. The equation for the one - dimensional convolutional layer is presented as follows:

$$c^l = \sum_{i=0}^{m} \left(w_i^l x_i^l \right) + b^l \tag{9}$$

where w^l and b^l are the weights and biases of the l layers and m is the convolution kernel size.

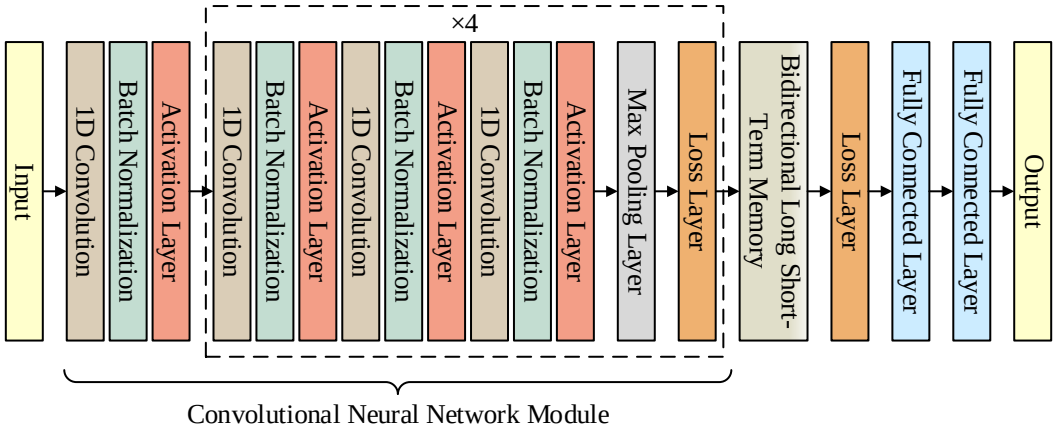

Figure 1: Structure of CNN-BLSTM

The batch normalization layer has the ability to homogenize the data distribution and accelerate the network training process. Meanwhile, the activation layer can bring about a non - linear transformation and enhance the model's fitting capabilities. For these reasons, a batch normalization layer along with an activation layer are incorporated subsequent to each convolutional layer. As far as the activation layer is concerned, most of the researches use the ReLU activation function (Eq. (10)), according to its principle, it is known that ReLU changes all negative inputs to 0. However, there are negative values in the data during the network processing, which will lead to the loss of information, so the activation layer in this paper adopts a self-regularized mish activation function (Eq. (11)):

$$ReLU = \begin{cases} x, & x > 0 \\ 0, & x \le 0 \end{cases} \tag{10}$$

$$mish = x \times \tanh\left(\ln\left(1 + e^x \right) \right) \tag{11}$$

To preserve the crucial data within the ECG signal and simultaneously diminish the computational intricacy of the network, a max - pooling layer having a kernel dimension of 2 and a stride of 2 is incorporated subsequent to each convolutional block. Moreover, as the dropout layer can avert model overfitting by randomly eliminating certain information, a

dropout layer with a dropout rate of 0.1 is added after the max - pooling layer.

3.2.2 Two - way Long - and Short - term Memory Network Component IMPORTANT

Leveraging the superiority of the long short - term memory network for handling dynamic data, this paper employs a bidirectional long short - term memory network subsequent to a convolutional neural network to capture the contextual relationships within features. The bidirectional long short - term memory network is composed of two sub - networks: a forward LSTM and a reverse LSTM. Each of these sub - networks has an equal number of LSTM units. In this study, we set the number of these units to 128.An LSTM unit is made up of input gates, output gates, and forgetting gates. These gates have the ability to either incorporate or eliminate information by regulating the flow of information within the unit. As a result, the unit can gather information from the time sequence.

The calculation formula is as follows:

$$f_t = \sigma\left(w_f x_t + w_f h_{t-1} + b_f\right) \tag{12}$$

$$i_t = \sigma\left(w_i x_t + w_i h_{t-1} + b_i\right) \tag{13}$$

$$u_t = \tanh\left(w_u x_t + w_u h_{t-1} + b_u\right) \tag{14}$$

$$c_t = i_t \times u_t + f_t \times c_{t-1} \tag{15}$$

$$o_t = \sigma\left(w_o x_t + w_o h_{t-1} + b_o\right) \tag{16}$$

$$h_t = o_t \times \tanh\left(c_t\right) \tag{17}$$

where i_t , f_t , c_t , and o_t are input gate, forgetting gate, unit state, and output gate respectively, u_t is the state update, and σ is the sigmoid activation function.

Right after the bidirectional long - and short - term memory network module, there is a loss layer having a loss rate of 0.2. Subsequently, a fully connected layer containing 64 neurons is present. Eventually, the softmax function is employed to carry out the classification task for the five electrocardiogram (ECG) signal categories suggested by the AAMI standard:

$$P\left(X_i\right) = \frac{e^{X_i}}{\sum_{j=1}^{5} e^{X_j}} \tag{18}$$

where $P(X_i)$ is the predicted probability distribution of X_i belonging to all possible classes.

3.2.3 Parameter setting

The maximum number of rounds for network training is 80 and the batch size is 128. The Adam optimization function is employed to update the weights, commencing with an initial learning rate of 0.001. Subsequently, to accelerate the convergence of the model, the learning rate is decreased via the learning rate decay approach, where the decay ratio is set at 0.1.

3.3 Investigations and Examination of Outcomes IMPORTANT

3.3.1 Experimental data and pre-processing

During the electrocardiogram (ECG) signal acquisition procedure, a diverse range of noise, including baseline drift, intermediate frequency (IF) interference, and electromyographic disturbance, frequently gets mixed in. The existence of this noise can, to a certain degree, impact the accuracy of ECG classification. To suppress the noise and enhance the signal - to - noise ratio of ECG signals, it is necessary to conduct a filtering process on the data before inputting it into the neural network.In this paper, the wavelet approach is employed for noise reduction. Specifically, the wavelet coefficients are examined. Coefficients with relatively small absolute values are set to zero, while those with larger absolute values are either retained or shrunk. Subsequently, the processed wavelet coefficients are reconstructed to obtain a noise - cancelled signal.Figure 2 depicts the ECG signals before and after noise reduction using the wavelet method. From this figure, it is evident that the wavelet transform method effectively eliminates the noise while preserving the useful signal.

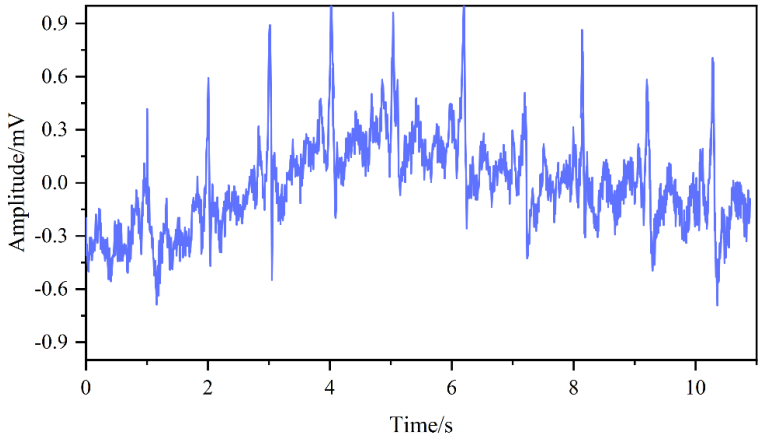

(a) Original signal

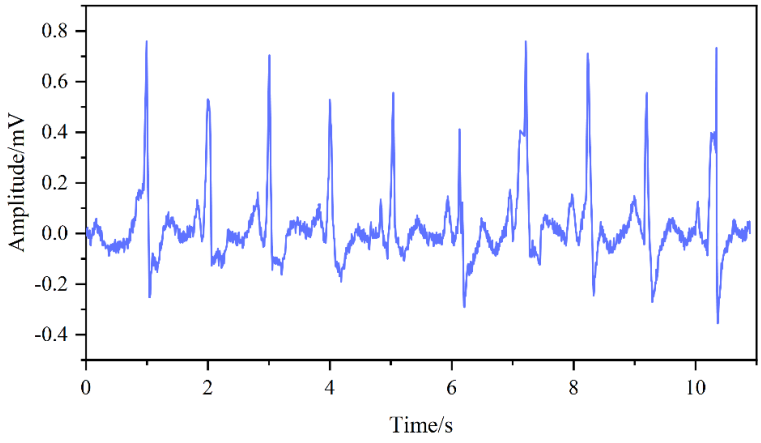

(b) The signal subsequent to wavelet noise reduction

Figure 2: Comparison of electrocardiogram (ECG) signals before and after noise reduction via the wavelet approach

The data employed in the experiment were sourced from the MIT - BIH arrhythmia database. This database was created by the Massachusetts Institute of Technology and contains 48 rhythm

signals, each 30 minutes long. These signals are from 47 subjects. A medical professional labeled them with 18 rhythm - type labels, and each signal was sampled at a frequency of 360 Hz.For the current article, the categorization criteria established by the American Association for the Advancement of Medical Instrumentation were utilized as a reference. A total of 96,289 asymmetric rhythms were classified into five main categories: normal (N), supraventricular (S), ventricular (V), fusion (F), and unknown (Q).The data underwent pre - processing. After the denoising procedure, 300 sampling points were chosen to create the dataset samples. Eighty percent of these data samples were used for training the network model. Given that this dataset was highly imbalanced, the ADASYN algorithm was applied to expand the small - category training set to the same scale. The remaining 20% of the dataset was reserved for validation, and the training and validation datasets were mutually independent with no overlap.

3.3.2 Assessment Approach Crucial

During this experiment, a set of four assessment measures is employed to conduct a comprehensive evaluation of the model's performance,namely, overall accuracy OA, precision η_P, recall η_r, and $F_{1-score}$, with the formulas defined as shown in Eqs. (19) to (22), and computed using a confusion matrix.

$$OA = \frac{T_P + T_N}{T_P + T_N + F_P + F_N} \tag{19}$$

$$\eta_p = \frac{T_P}{T_P + F_P} \tag{20}$$

$$\eta_r = \frac{T_P}{T_P + F_N} \tag{21}$$

$$F_{1-score} = \frac{\left(1+\beta^2\right)\cdot \eta_p \cdot \eta_r}{\beta^2 \cdot \eta_p + \eta_r} \tag{22}$$

Here, T_P represents the true positive. It denotes the quantity of rhythm samples. These samples have a positive true category and are also classified as positive. ; F_N is false negative, indicating the number of rhythm samples whose true category is positive that are classified as negative; T_N is true negative, indicating the number of rhythm samples whose true category is negative that are classified as negative; F_P is a false positive, indicating the number of heart rhythm samples whose true category is negative that are categorized as positive; β serves as a coefficient employed to modify the relative significance of precision in comparison to recall. Typically, it is regarded as $\beta = 1$, at which point Eq. (22) is:

$$F_{1-score} = \frac{2\cdot \eta_p \cdot \eta_r}{\eta_p + \eta_r} \tag{23}$$

3.3.3 Experimental results

The investigations were carried out by utilizing the TensorFlow deep - learning architecture, based on the Python language, calling the Keras library. All experimental studies were done on

a computer with CPU: Intel(R) Core(TM) i5-7300HQ CPU@2.50GHz, GPU: NVIDIA GeForce GTX 1050, and Windows 11 operating system. Figure 3 shows the training and testing performance of 130 iterations completed using conventional CNN network as well as CNN-BiLSTM network respectively.

As can be concluded from the figure, both have better performance. The test set of the model using only traditional CNN for feature extraction obtained 98.94% accuracy while the model using CNN-BiLSTM network achieved 99.58% accuracy of the test set in the same period.

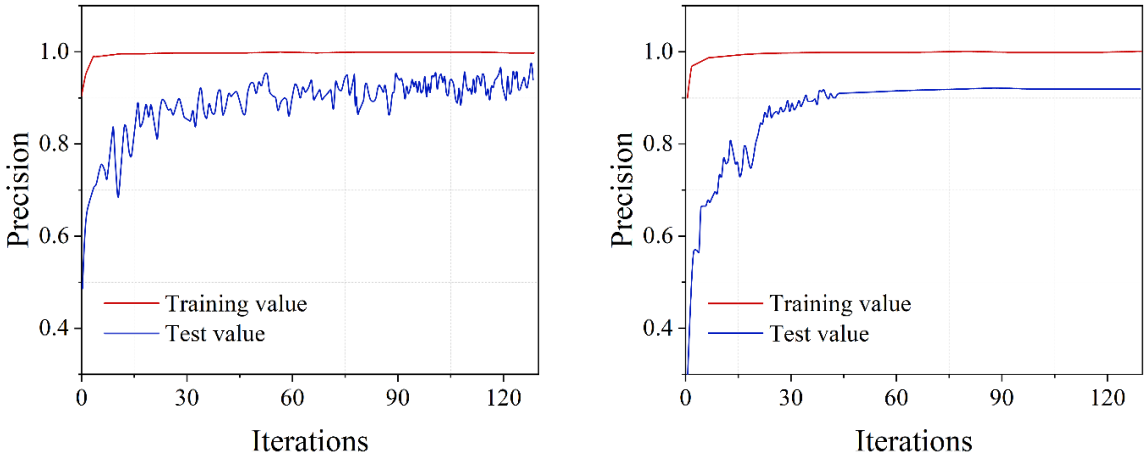

(a) CNN (b) CNN-BiLSTM

Figure 3: Network training and test performance charts

Under the same experimental conditions detailed above, a comparison is made between the conventional CNN network and the enhanced CNN - BiLSTM network. Table 1 presents the values obtained for the evaluation indices of each of the two distinct network models.

The values of the assessment indices for classes S and F in the two models are comparatively low. Meanwhile, the CNN-BiLSTM network shows different degrees of improvement in all types of evaluation indexes, especially in classes S and F. The precision and recall of class S are improved by 2.02% and 9.65%, and those of class F are improved by 12.94% and 4.11%, This suggests that the model is enhanced on the basis of the CNN model. The CNN model itself has been refined, and an improved CNN - BiLSTM network has also been involved in this improvement process. The efficacy of the model after the enhancement made on the foundation of the CNN model.

Table 1: CNN network and CNN-BiLSTM network relevant evaluation indicators (%)

Network model	Evaluating indicator	Cardiac rhythms				
		N	S	V	F	Q
CNN	η_P	99.23	89.75	97.14	77.35	99.17
	η_r	99.23	82.53	98.02	89.47	99.34
	$F_{1-score}$	99.23	86.09	97.59	83.36	99.51
CNN-BiLSTM	η_P	99.71	91.77	98.83	90.29	99.88
	η_r	99.69	92.18	98.37	93.58	99.88
	$F_{1-score}$	99.70	92.22	98.62	91.81	99.88

The confusion matrix for the test set is presented in Figure 4, and Table 2 showcases a

comparison of the outcomes of two evaluation metrics. By examining the data in the table, we can observe that the CNN network achieves an overall accuracy of 98.91% when applied to 18932 rhythm data. Specifically, its precision and recall rates stand at 94.18% and 93.08% respectively.In contrast, the CNN - BiLSTM network demonstrates superior performance on the test - set data. This model attains an overall accuracy of 99.13%. Moreover, its precision and recall values surpass those of the CNN network, reaching 97.33% and 96.47% respectively. The F1 - score, a comprehensive metric, also indicates that the CNN - BiLSTM network outperforms the CNN model, suggesting greater robustness.It is also worth noting that there is no overlapping data between the training set and the test set in this experiment. This absence of duplicate data validates the model's high adaptability in classifying arrhythmias.

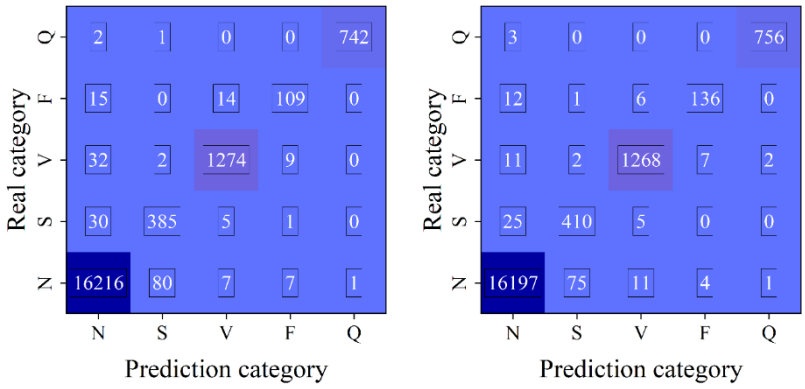

(a) CNN (b) CNN-BiLSTM

Figure 4: Network model test set confusion matrix

Table 2: CNN network and CNN-BiLSTM network evaluation indicators (%)

Network model	OA	η_P	η_r	$F_{1-score}$
CNN	98.91	94.18	93.08	93.29
CNN-BiLSTM	99.13	97.33	96.47	96.92

The effectiveness of the CNN - BiLSTM model is contrasted against other arrhythmia classification models on the basis of the MIT - BIH dataset. These alternative models encompass LSTM, BiLSTM, and CNN, and the data of each index of the classification results are specifically shown in Table 3.

It can be learned that the proposed CNN-BiLSTM model has certain advantages over other models in realizing automatic classification of ECG signals. The overall accuracy reaches 99.46%, which is higher than the corresponding value of other methods; the precision reaches 96.53%, which is slightly higher than the 95.21% of BiLSTM; the recall is slightly lower than BiLSTM, Moreover, there is the F1 - score metric. This metric represents the mean value obtained from the harmonization of the accuracy (precision) and the retrieval rate (recall), reaches 95.99%, which is also second only to the corresponding value of LSTM, and better than BiLSTM and CNN's corresponding values, which is at a better level.

Table 3: Comparison of performance indexes of classification results of arrhythmia

Algorithm	Signal length	Function /%			
		OA	η_P	η_r	$F_{1-score}$
LSTM	250samples	94.18	97.99	96.85	97.41
BiLSTM	75×75	96.19	95.21	72.22	82.49
CNN	270 samples	98.85	92.74	94.58	93.67
CNN-BiLSTM	300 samples	98.96	93.59	92.51	92.92
		99.46	96.53	95.72	95.99

4 Prediction of blood pressure trends based on CNN-LSTM with PPG signals

4.1 PPG signal preprocessing

4.1.1 PPG signal labeling

In this research, arterial blood pressure (ABP) signals and photoplethysmogram (PPG) signals measured via radial artery catheterization were employed for the evaluation and categorization of hypertension. These signals were sourced from the MIMIC - III critical care database. In this article, only the PPG signal and ABP signal data served as the primary data sources.To accurately acquire blood pressure labels, signal records that were unusable, such as those with missing peaks, bimodal pulses, or no signal at all, were excluded from the study. Ultimately, recordings were gathered from 124 subjects. Each recording had a duration of 130 seconds and a sampling frequency of 145 Hz.Each recording included an ABP signal as the target source and a PPG signal as the predictor source. Subsequently, these recordings were divided into 5 - second signal segments. This segmentation method has been proven effective for obtaining information related to heartbeat cycles.

4.1.2 PPG-derived signal extraction and denoising

The photoplethysmogram (PPG) signals underwent primary and secondary differentiation processes. As a result, first - and second - order derivative signals were acquired. These derivative signals respectively stand for the velocity pulse wave (VPG) and the acceleration pulse wave (APG).The acquired signals are inevitably interfered by environmental and physiological factors (e.g., IFI, baseline drift, and multi-scene motion artifacts) due to noise contamination of the acquired signals, either manually or by machine equipment. Therefore, noise reduction of the signal is an essential step.

4.2 PPG signal feature extraction

In this paper, we will use the Tsfresh method in the Python package for feature extraction of signal segments, Tsfresh, a feature engineering instrument designed for relational databases handling time - series data, offers 77 techniques for characterizing time series. A grand total of 794 time - series characteristics are present, which depict fundamental traits like the crests, means or maxima of a time series, as well as time complex features such as inverse symmetry statistics.

In this paper, Simultaneously, several time series sub - segments accompanied by classification labels y are fed into the Tsfresh function. Subsequently, the numerical characteristics of these time series sub - segments are extracted, so that 794 features are

extracted from each time series subsection respectively, and then the features that do not have a significant impact on the recognition results are further filtered out according to the label value of y, and 189 features are obtained for each PPG time series subsection, each VPG time series subsection 200 features are obtained, and 190 features are obtained for each APG temporal sub-segment.

Six Tsfresh feature extraction methods are listed below:

(1) $abs\_energy(x)$: absolute energy value, the absolute energy of the time - series data, which is the sum of the squared values, is what this refers to.:

$$E = \sum_{i=1,\cdots,n} x_i^2 \tag{24}$$

(2) $cwt\_coefficients(x, param)$: Ricker wavelet analysis, which refers to the continuous wavelet transform of signal data based on the Ricker wavelet:

$$cwt = \frac{2}{\sqrt{3a}\pi^{\frac{1}{4}}}\left(1-\frac{x^2}{a^2}\right)\exp\left(-\frac{x^2}{2a^2}\right) \tag{25}$$

(3) $fft\_coefficient(x, param)$: Fourier transform coefficients are the values of a one - dimensional discrete Fourier series. These coefficients are calculated using the Fast Fourier Transform algorithm for time - series data:

$$A_k = \sum_{m=0}^{n-1} a_m \exp\left\{-2\pi i \frac{mk}{n}\right\}, k = 0,\cdots,n-1 \tag{26}$$

(4) $mean\_abs\_change(x)$: the absolute mean change value, which refers to the average of the absolute differences between the time series data:

$$A_{ac} = \frac{1}{n-1}\sum_{i=1,\cdots,n-1}\left|x_{i+1}-x_i\right| \tag{27}$$

(5) $mean\_second\_derivative\_central(x)$: the central mean of the second-order derivative, This pertains to the mean of the central estimation of the second - order derivative of the time - sequence data:

$$A_d = \frac{1}{2(n-2)}\sum_{i=1,\cdots,n-2}\frac{1}{2}\left(x_{i+2}-2\cdot x_{i+1}+x_i\right) \tag{28}$$

(5) $time\_reversal\_asymmetry\_statistic(x, lag)$: the central mean of the second-order derivative, which refers to the average of the central approximation of the second-order derivative of the time series data:

$$A_t = \frac{1}{n-2lag}\sum_{i=1}^{n-2lag} x_{i+2lag}^2 \cdot x_{i+lag} - x_{i+lag}\cdot x_i^2 \tag{29}$$

4.3 Prediction of blood pressure using CNN - LSTM network models

4.3.1 CNN-LSTM network model architecture

The CNN-LSTM network model consists of a front-end CNN network and a back-end LSTM network.The CNN network is able to automatically perform feature extraction on the image, avoiding the problem of difficult waveform feature extraction from different samples due to physiological differences, and ignoring the effect of tiny noise information.The LSTM network integrates the deep matrix output from the CNN network, summarizes the sequence feature quantity, and utilizes the LSTM network's cyclic chain structure to get the relevant time series information to assist the model for prediction.

4.3.2 Network Model Tuning

In this segment, the architecture of the CNN - LSTM network is refined to boost the algorithm's performance. This is achieved by integrating the attention mechanism and modifying the LSTM configuration.

The CBAM module serves as an attention mechanism that aims to strengthen the feature representation capacity of convolutional neural networks, which strengthens the feature map representation ability through adaptive spatial and channel attention mechanisms, making the CNN model more accurate and robust.The main advantage of CBAM module is that it can improve the representation ability of CNNs without increasing the complexity of the network. Moreover, the CBAM module is easy to be embedded into any CNN to improve the network performance due to its generalized structure.

BiLSTM network extends the capability of the model by adding the structure of back-passing on top of LSTM. Specifically, BiLSTM inputs the output of the LSTM model into the LSTM model one more time by means of reverse pass, and then combines the outputs of forward pass and reverse pass to obtain a more comprehensive information representation. This configuration enables BiLSTM to detect dependencies in both the forward and backward directions within time - series data. As a result, it boosts the model's capacity to represent information.

The CBAM-CNN-BiLSTM model is based on CNN-LSTM and combines the advantages of CBAM and BiLSTM modules to better process image and signal data.

4.3.3 Blood pressure forecasting

In this research, a total of 174,963 signal segments were acquired from 1741 participants. Subsequently, the dataset was randomly partitioned into two subsets, with 80% and 20% of the data respectively. The training set consisted of 139,970 signal segments, while the test set contained 34,993 signal segments.The learning rate, a crucial hyperparameter in the deep - learning model, controls the alterations in network weights based on the loss gradient of the optimization algorithm. This has an influence on the speed of model training. In this study, a dynamic learning rate is implemented. Specifically, if the system detects that the Mean Absolute Error (MAE) of the validation group does not decline over 100 consecutive training rounds, the learning rate is automatically reduced by multiplying it with 0.96.This dynamic learning rate mechanism helps to ensure the long - term stability of the model. Here, the initial learning rate is set at 10 - 3, and the lower bound of the learning rate is set to 0.

4.4 Findings from Experiments and Their Analysis

4.4.1 Short-term forecast results and analysis

Figure 5 depicts the systolic blood pressure (SBP) and diastolic blood pressure (DBP) forecasts generated by the blood pressure prediction model founded on the CNN+LSTM network. As can be gleaned from the figure, when the CNN network is integrated with the LSTM for blood pressure prediction, the error in the predicted DBP value is minimal. In contrast, the discrepancy between the predicted and actual values of SBP is somewhat larger.

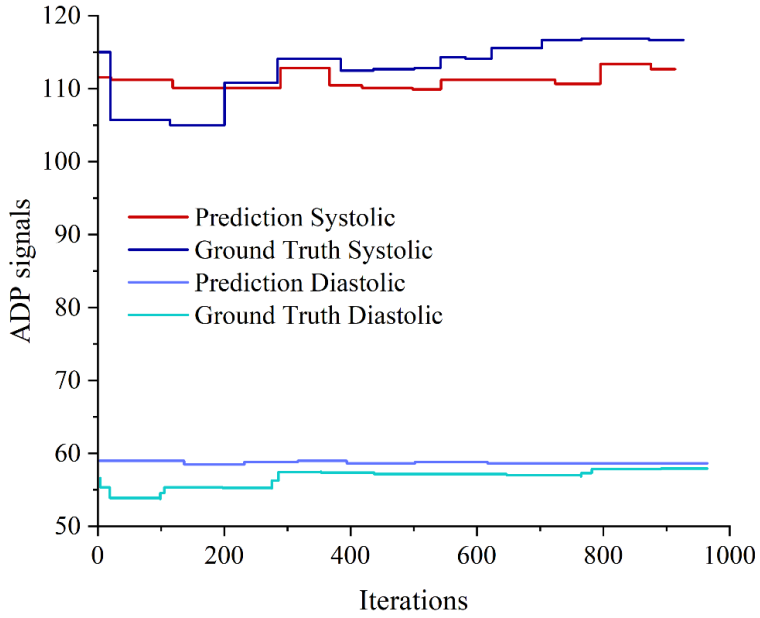

Figure 5: SBP and DBP Prediction Model Based on CNN+LSTM

The Bland - Altman graphs depicting the systolic blood pressure (SBP) and diastolic blood pressure (DBP) for this forecasting model are presented in Figures 6 and 7. In the prediction results of this model, the mean line of SBP is -3.89, and the mean line of DBP is 0.52. Although the error of more than 96% of the points can also be kept within the interval of ±2.09 STD, In comparison to the LSTM - based model, the mean line of this model is farther from 0. As a result, the consistency of this model is marginally lower than that of the LSTM model.

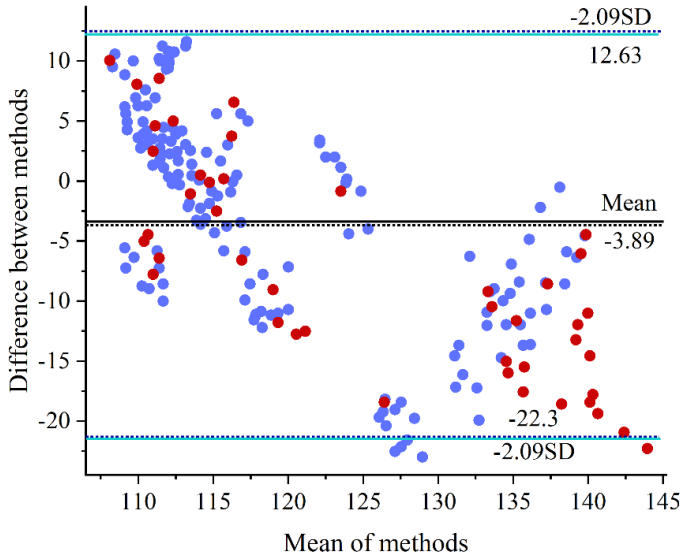

Figure 6: Bland-Altman plot of SBP

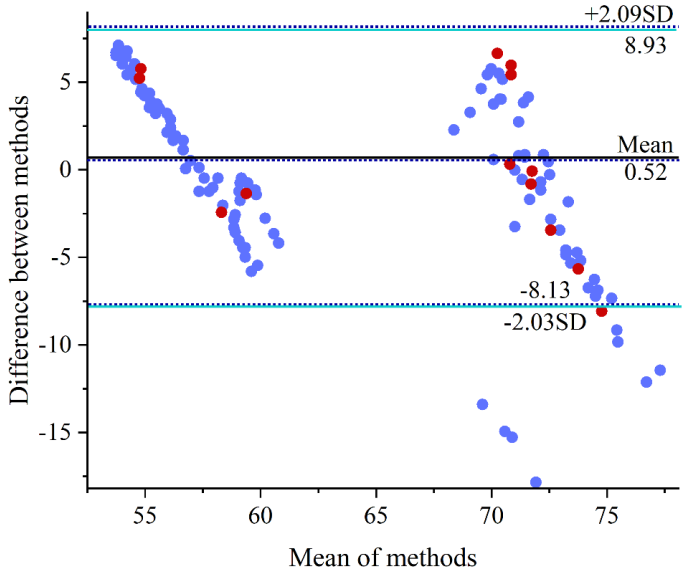

Figure 7: Bland-Altman plot of DBP

4.4.2 Results and Analysis of Multi-stage Blood Pressure Prediction

Figure 8 presents the histogram depicting the error distribution of the final outcomes of the multistage model. This model was built using a combination of Convolutional Neural Network (CNN) and Long Short - Term Memory (LSTM) for predicting systolic and diastolic blood pressure. Based on the information in the figure, the final results are presented as shown in Table 4, the multi-stage model of CNN plus LSTM has a systolic ME of 0.8429 mmHg, MAE of 4.5916 mmHg, RMSE of 7.1219 mmHg, and STD of 7.0248 mmHg with a correlation coefficient of 0.95188.The predicted diastolic ME was 0.9741 mmHg, the MAE was 2.2577 mmHg, RMSE was 3.0081 mmHg, and STD was 2.9155 mmHg with a correlation coefficient of 0.96726.

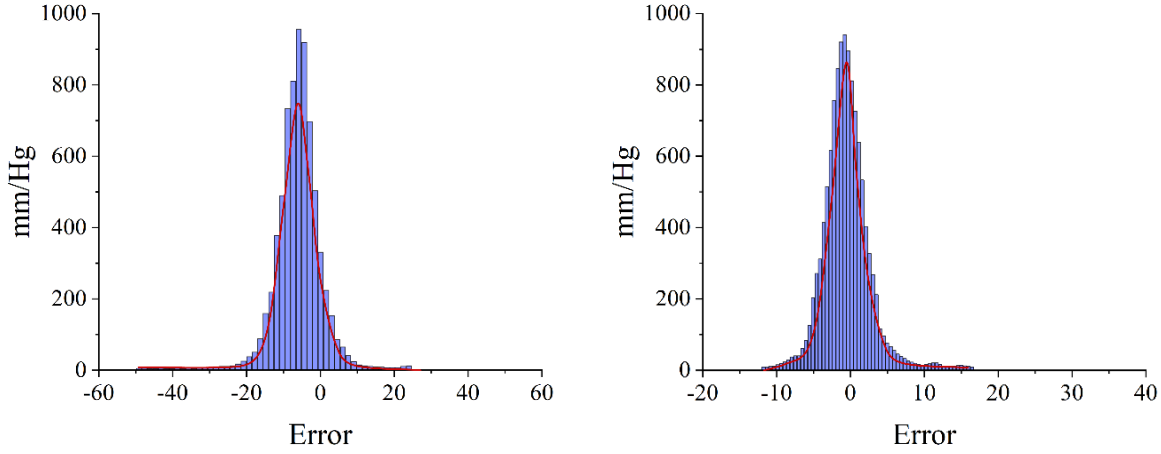

(a) Systolic pressure (b) Diastolic pressure

Figure 8: Histogram of final error distribution of CNN+LSTM model

Table 4: CNN-LSTM model for prediction of systolic and diastolic blood pressure assessment

	ME (mm/Hg)	MAE (mm/Hg)	RMSE (mm/Hg)	STD (mm/Hg)	Correlation coefficient
Systolic pressure	0.8429	4.5916	7.1219	7.0248	0.95188
Diastolic pressure	0.9741	2.2577	3.0081	2.9155	0.96726

Figure 9 presents the regression plots for systolic and diastolic blood pressure. Based on the experimental outcomes, it is evident that the integrated model outperforms the individual CNN and LSTM models in terms of prediction precision. However, the prediction precision for systolic blood pressure is marginally lower than that of the enhanced VGG19 model, whereas the prediction precision for diastolic blood pressure is higher, so it can be concluded that both acquiring features with higher dimensional abstraction and capturing temporal dependence can improve the prediction accuracy of blood pressure, but acquiring features with higher dimensional abstraction makes a greater contribution to improving the prediction accuracy than capturing temporal dependence contributes more to improving prediction accuracy.

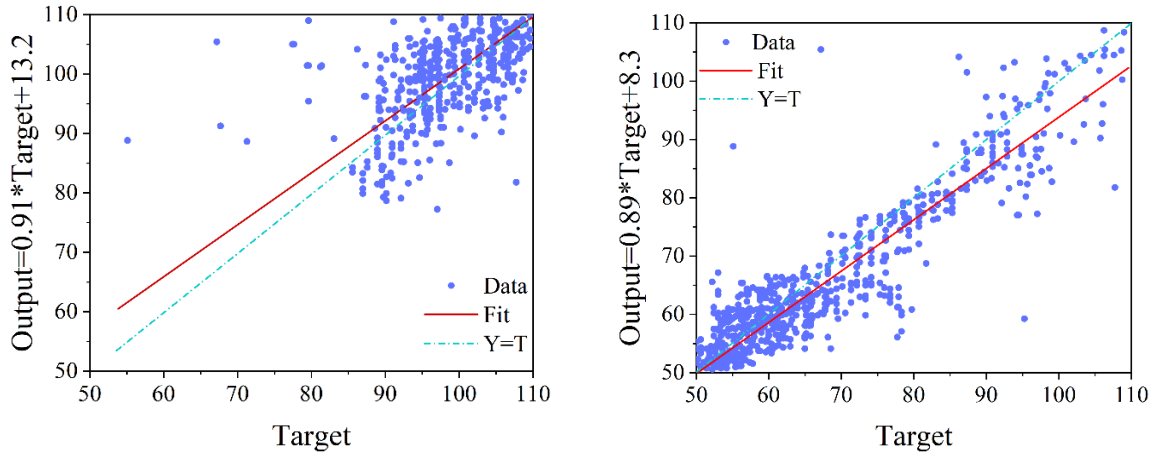

(a) Systolic pressure (b) Diastolic pressure

Figure 9: Regression plot of CNN+LSTM model prediction results

5 Design of wearable ECG monitoring system

5.1 Design of the Overall System Framework

The comprehensive structure of the system devised in this paper is split into three components: the signal collection unit, the local surveillance unit, and the interactive presentation unit. The design of the overall system framework is presented in Figure 10.

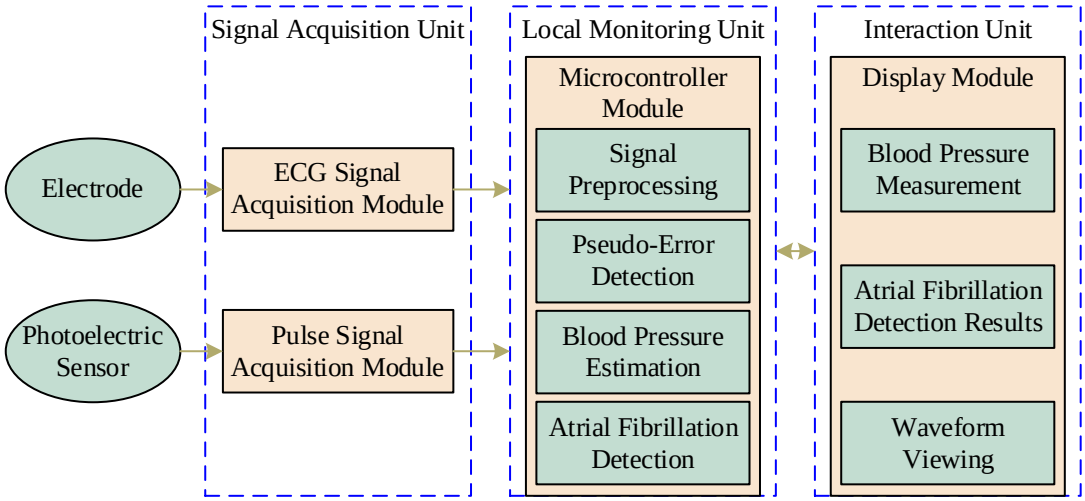

Figure 10: System Framework

5.2 System technical design

5.2.1 System key technologies

(1) ECG signal acquisition technology

Owing to the feeble, low - frequency, and haphazard nature of the electrocardiogram (ECG) signal, to acquire top - quality ECG signals, the design of the ECG signal acquisition circuit demands high - level specifications like high amplification, high common - mode rejection rate, and high input resistance.

Since the ECG signal is extremely weak (mv scale) and accompanied by noise and interference, the collected ECG signal needs to be filtered, amplified and other pre-processing. In order to reduce the volume and ensure the stability of the collected signal, this paper adopts the analog front-end chip ADS1292 developed by TI, which integrates most of the functions required for the front-end of the ECG acquisition, that is, only need to join the filter circuit at the front end to complete the acquisition and pre-processing of ECG signals.

(2) Pulse signal acquisition technology

Waves around 560nm wavelength can reflect the information of micro-arteries in shallow parts of the skin, which is very suitable for extracting pulse signals. The photoelectric volumetric pulse tracing method is characterized by easy measurement method, convenient wearing, and high reliability of acquisition, so this technology is often applied to the blood pressure measurement of wearable devices.

(3) Selection of microcontroller

In order to achieve a highly integrated circuit design, this paper chooses a microcontroller with its own A/D conversion function, in addition to the convenience of pulse wave analog signal to digital signal conversion, while taking into account the algorithms in the microcontroller floating-point mathematical operations, which is when microcontroller

selection is very important.

5.2.2 Blood pressure trend prediction techniques

Considering the engineering implementation of algorithms in wearable devices, data-driven blood pressure measurement methods based on other methods have limited application scenarios and are not suitable for the research of the monitoring system in this paper due to their poor interpretability and lack of powerful arithmetic chip support. Since the blood pressure physiological estimation model has good interpretability for the physiological mechanism of blood pressure, for example, CNN-LSTM can track the change of blood pressure for a long time, and the morphological features of the pulse signal can respond to certain vascular elasticity information, etc., in addition, the computational workload of feature extraction is comparatively straightforward. As a result, this research paper employs an approach that integrates CNN - LSTM with pulse wave features to build the blood pressure estimation model.

5.2.3 Real-time arrhythmia monitoring technology

Since the AF detection method based on atrial activity is sensitive to noise and not applicable to wearable devices, the CNN-BiLSTM-based AF detection method is the mainstream for wearable devices. After further consideration, the CNN-BiLSTM-based AF detection algorithm is selected in this paper, which also provides a feasible solution for recognizing AF based on ECG signals collected by wearable devices.

5.3 System Hardware Design

(1) ECG signal acquisition module

The ECG acquisition module in this paper is mainly an integrated circuit module composed of ADS1292 front-end analog chip. The working principle of the circuit is mainly through high-frequency filtering, impedance matching and other means, its internal integration of multi-stage amplification circuit and filter conditioning circuit, so the acquisition of the human ECG signal of high quality, and the module internal integration of high-resolution ADC converter at the same time, only through the software mode can be conveniently realized by the high quality of the reception of ECG data.

(2) Pulse wave signal acquisition module

This paper's pulse wave acquisition module is mainly pulse sensor sensor composed of integrated circuit module, the module is composed of LED light source and photoelectric conversion sensor two parts, the method of use through the strap and other fixed methods in the wearer's finger tips or earlobes.

(3) Microcontroller circuit module

The microcontroller specifically used in this paper is STM32F407, the primary clock speed of the central processing unit is 168 megahertz, the microcontroller is a chip based on Cortex™-M4 core. Since its main frequency is 168 MHz, it is possible to achieve zero flash wait using the designed ART gas pedal. Its built-in digital processing instructions and floating-point calculation unit expand the chip's range of applications.

(4) Display circuit module

Since the initialization of the system requires human-computer interaction operations, such as initializing the blood pressure estimation model, viewing the collected ECG data and viewing the report information of the system for the past day, the display module designed in this paper is an LCD with resistive touch function and its resolution is 320*240.

6 Conclusion

This paper presents a composite model for the real - time detection of arrhythmia. The model combines a convolutional neural network and a bidirectional long - short - term memory network (CNN - BiLSTM). To optimize the CNN - BiLSTM model, an attention mechanism is incorporated. For the blood pressure prediction experiments, root mean square error (RMSE), mean absolute error (MAE), and the Bland - Altman plot are chosen as the model evaluation metrics.The research findings indicate that the CNN - BiLSTM network achieves a classification accuracy of 99.46%. Additionally, the precision and recall rates are as high as 97.33% and 96.47% respectively. This suggests that the proposed model in this paper has significantly improved compared to the original model in terms of accuracy and other relevant aspects. It also enables the real - time detection of cardiac arrhythmia.Regarding blood pressure prediction, the optimized CNN - BiLSTM model shows a marginal improvement in the prediction performance of systolic blood pressure, while there is a slight decline in the prediction performance of diastolic blood pressure.Based on these research results, a wearable system for the synchronized monitoring of dynamic blood pressure and atrial fibrillation was designed.

Funding

This research was supported by the 2024 Fujian Provincial Key Project of Vocational and Lifelong Education (Intelligent Embedded Control Technology); 2024 Fujian Provincial Domestic Visiting Scholar Program for Higher Education Institutions; 2024 Discipline Construction and Teaching Reform Project of Fujian Health College (JG2024112).

References

[1] Conrad, N., Molenberghs, G., Verbeke, G., Zaccardi, F., Lawson, C., Friday, J. M., ... & McMurray, J. J. (2024). Trends in cardiovascular disease incidence among 22 million people in the UK over 20 years: population based study. Bmj, 385.

[2] McAloon, C. J., Osman, F., Glennon, P., Lim, P. B., & Hayat, S. A. (2016). Global epidemiology and incidence of cardiovascular disease. In Cardiovascular Diseases (pp. 57-96). Academic Press.

[3] Rege, S., Barkey, T., & Lowenstern, M. (2015, March). Heart arrhythmia detection. In 2015 IEEE Virtual Conference on Applications of Commercial Sensors (VCACS) (pp. 1-7). IEEE.

[4] Gupta, V., Mittal, M., & Mittal, V. (2020). Chaos theory: an emerging tool for arrhythmia detection. Sensing and Imaging, 21(1), 10.

[5] Luz, E. J. D. S., Schwartz, W. R., Cámara-Chávez, G., & Menotti, D. (2016). ECG-based heartbeat classification for arrhythmia detection: A survey. Computer methods and programs in biomedicine, 127, 144-164.

[6] Sannino, G., & De Pietro, G. (2018). A deep learning approach for ECG-based heartbeat classification for arrhythmia detection. Future Generation Computer Systems, 86, 446-455.

[7] Abdelrazik, A., Eldesouky, M., Antoun, I., Lau, E. Y., Koya, A., Vali, Z., ... & Ng, G. A. (2025). Wearable devices for arrhythmia detection: advancements and clinical implications. Sensors (Basel, Switzerland), 25(9), 2848.

[8] Sajeev, J. K., Koshy, A. N., & Teh, A. W. (2019). Wearable devices for cardiac arrhythmia detection: a new contender?. Internal medicine journal, 49(5), 570-573.

[9] Bokhari, S. F. H., Waseem, A. B., Raza, H., Iqbal, A., Javaid, S., Idrees, B., ... & Dost, W. (2025). Advancing cardiac arrhythmia management: The integration of wearable technology and remote monitoring. World Journal of Cardiology, 17(7), 106841.

[10] Cheung, C. C., Krahn, A. D., & Andrade, J. G. (2018). The emerging role of wearable technologies in detection of arrhythmia. Canadian Journal of Cardiology, 34(8), 1083-1087.

[11] Ip, J. E. (2019). Evaluation of cardiac rhythm abnormalities from wearable devices. JAMA, 321(11), 1098-1099.

[12] Liu, J., Li, Z., Jin, Y., Liu, Y., Liu, C., Zhao, L., & Chen, X. (2022). A review of arrhythmia detection based on electrocardiogram with artificial intelligence. Expert review of medical devices, 19(7), 549-560.

[13] Neri, L., Oberdier, M. T., Van Abeelen, K. C., Menghini, L., Tumarkin, E., Tripathi, H., ... & Halperin, H. R. (2023). Electrocardiogram monitoring wearable devices and artificial-intelligence-enabled diagnostic capabilities: a review. Sensors, 23(10), 4805.

[14] Wu, Y. C., & Feng, J. W. (2018). Development and application of artificial neural network. Wireless Personal Communications, 102(2), 1645-1656.

[15] Abiodun, O. I., Jantan, A., Omolara, A. E., Dada, K. V., Mohamed, N. A., & Arshad, H. (2018). State-of-the-art in artificial neural network applications: A survey. Heliyon, 4(11).

[16] Alber, M., Lapuschkin, S., Seegerer, P., Hägele, M., Schütt, K. T., Montavon, G., ... & Kindermans, P. J. (2019). iNNvestigate neural networks!. Journal of machine learning research, 20(93), 1-8.

[17] Bollepalli, S. C., Sevakula, R. K., Au-Yeung, W. T. M., Kassab, M. B., Merchant, F. M., Bazoukis, G., ... & Armoundas, A. A. (2021). Real-time arrhythmia detection using hybrid convolutional neural networks. Journal of the American Heart Association, 10(23), e023222.

[18] Crea, F. (2021). The growing role of artificial intelligence and of wearable devices in the management of arrhythmias. European Heart Journal, 42(38), 3889-3893.

[19] Ali, N. F., & Atef, M. (2023). An efficient hybrid LSTM-ANN joint classification-regression model for PPG based blood pressure monitoring. Biomedical Signal Processing and Control, 84, 104782.

[20] Joseph, T., & TS, B. (2024). Real-time Blood Pressure Prediction on Wearables with Edge-Based DNNs: A Co-Design Approach. ACM Transactions on Design Automation of Electronic Systems, 30(1), 1-24.